Characterization of Compositional Changes in Vacuum Gas Oil Distillation Cuts by Electrospray Ionization Fourier Transform–Ion Cyclotron Resonance (FT–ICR) Mass Spectrometry

ARTICLE *in* ENERGY & FUELS · JUNE 2006

Impact Factor: 2.79 · DOI: 10.1021/ef060104g

4 AUTHORS, INCLUDING:

Sunghwan Kim
Kyungpook National University
66 PUBLICATIONS **2,224** CITATIONS

SEE PROFILE

Characterization of Compositional Changes in Vacuum Gas Oil Distillation Cuts by Electrospray Ionization Fourier Transform−Ion Cyclotron Resonance (FT−ICR) Mass Spectrometry

Lateefah A. Stanford,[†] Sunghwan Kim,[‡] Ryan P. Rodgers,[‡] and Alan G. Marshall*[,†,‡]

Department of Chemistry and Biochemistry, Florida State University, Tallahassee, Florida 32306, and National High Magnetic Field Laboratory, Florida State University, 1800 East Paul Dirac Drive, Tallahassee, Florida 32310-4005

Received March 10, 2006. Revised Manuscript Received May 8, 2006

We present the acidic polar heteroatomic molecular class composition of three distillate fractions (light, 563−606 °F; middle, 606−853 °F; and heavy, 853−1009 °F) of a vacuum gas oil (VGO). Acidic and basic species were detected by high-resolution negative-ion and positive-ion electrospray ionization (ESI) Fourier transform−ion cyclotron resonance mass spectrometry (FT−ICR MS). Each distillate was exhaustively characterized by mass, heteroatom class, type (rings plus double bonds), and carbon number distribution to mark compositional trends with increased distillation temperature. The light distillate fraction exhibits monoaromatic and low double-bond equivalence (DBE) polycyclic species. Low-molecular-weight polycyclic and monoaromatic carboxylic acids and oxygen−sulfur (S_xO_y) species solely populate the negative-ion mass spectrum of the light distillate. In contrast, the middle and heavy distillates are composed of high-molecular-weight and high-DBE polyaromatic species such as pyrrolic and phenolic species, in addition to polyaromatic carboxylic acids. Light and middle distillate carboxylic acids and O_xS species fractionate by alkyl chain length but not by DBE value.

Introduction

Saudi Arabia accounts for 26% of the world's known oil reserves. The Jurassic carbonate, Cretaceous, and Paleozoic reserves of Saudi Arabia comprise billions of barrels of sweet light crude oil.[1] Middle Eastern sweet crude oil remains a high-value commodity because of its low heteroatom and impurity content. In contrast, heavy crude oils have a high heteroatom content and are less desirable. Heavy crude oils require extensive downstream processing to remove heteroatomic species that contribute to fouling in hydrocarbon streams, corrosion, and NO_x and SO_x emissions during combustion.[2] Sole reliance on Middle Eastern sweet crude oil will result in a steady increase in the cost of petroleum exportation to its neighbors. As the supply of light sweet Middle Eastern crude oils is exhausted, reliance will shift to highly acidic heavy oils that are high in heteroatoms from the United States, China, eastern Europe, and Venezuela. Consequently, catalytic hydrotreatment becomes increasingly essential.

Lack of knowledge of the chemical reactivity and properties of polar crude oil heteroatomic species limits future gains in refining efficiency. Adverse effects such as polymerization, auto-oxidation, corrosion, and thermal composition all derive from molecular composition.[2] Acidic nitrogen-containing classes (pyrrolic) in middle distillates impair catalytic hydrodesulfurization, via coke formation at the catalyst surface.[3−5] Moreover, pyrrolic species resist catalytic hydrotreatment, and oxygenated species hamper the distillation process and corrode metal surfaces during distillation. A typical distillation scheme includes preheating and desalting, topping, stabilization, atmospheric distillation, and vacuum distillation to produce liquid petroleum gas, naphtha, jet fuel, kerosene, diesel, and light and heavy vacuum gas oils (VGOs).[6,7] Corrosion at high fluid velocity and high temperature by naphthenic acids and acidic sulfur compounds during distillation destroys transfer lines, furnace tubes, valves, and pump fittings.[5,8]

Petroleomic research seeks to correlate chemical properties and behavior with the chemical composition of fossil fuels.[3,9] High mass resolution is essential for accurate and complete compositional analysis, because the relative abundance dynamic

* To whom correspondence should be addressed.
[†] Department of Chemistry and Biochemistry.
[‡] National High Magnetic Field Laboratory.

(1) Cole, G. A.; Abuali, M. A.; Aoudeh, S. M.; Carrigan, W. J.; Chen, H. H.; Colling, E. L.; Gwathney, W. J.; Alhajii, A. A.; Halpern, H. I.; Jones, P. J.; Alsharidi, S. H.; Tobey, M. H., Organic Geochemistry of the Paleozoic Petroleum System of Saudi-Arabia. *Energy Fuels* **1994**, *8* (6), 1425−1442.

(2) Watkinson, A. P.; Navaneetha-Sundaram, B.; Posarac, D. Fouling of a sweet crude oil under inert and oxygenated conditions. *Energy Fuels* **2000**, *14* (1), 64−69.

(3) Marshall, A. G.; Rodgers, R. P. Petroleomics: The next grand challenge for chemical analysis. *Acc. Chem. Res.* **2004**, *37* (1), 53−59.

(4) Snyder, L. R. Nitrogen and Oxygen Compound Types in Petroleum. Total Analysis of an 850−1000 °F Distillate from a California Crude Oil. *Anal. Chem.* **1969**, *41* (8), 1084-1094.

(5) Wu, X. Q.; Jing, H. M.; Zheng, Y. G.; Yao, Z. M.; Ke, W. Erosion-corrosion of various oil-refining materials in naphthenic acid. *Wear* **2004**, *256* (1−2), 133−144.

(6) Rivero, R.; Rendon, C.; Gallegos, S., Exergy and exergoeconomic analysis of a crude oil combined distillation unit. *Energy* **2004**, *29* (12−15), 1909−1927.

(7) Voelkel, A.; Fall, J., Inverse gas chromatography for the examination of fractions separated from oil vacuum distillation residues. *J. Chromatogr., A* **1997**, *768* (2), 271−281.

(8) Hughey, C. A.; Rodgers, R. P.; Marshall, A. G.; Qian, K. N.; Robbins, W. K. Identification of acidic NSO compounds in crude oils of different geochemical origins by negative ion electrospray Fourier transform ion cyclotron resonance mass spectrometry. *Org. Geochem.* **2002**, *33* (7), 743−759.

(9) Rodgers, R. P.; Schaub, T. M.; Marshall, A. G. Petroleomics: Mass Spectrometry Returns To Its Roots. *Anal. Chem.* **2005**, *77*, 20A−27A.

10.1021/ef060104g CCC: $33.50
Published on Web 06/21/2006

range of petroleum components is 10 000−100 000.[3] Conventional analytical techniques such as gas chromatography/mass spectroscopy (GC/MS) lack the necessary peak capacity (i.e., spectral range divided by the width of one peak). Thus, chemical derivatization, precipitation, chromatography, and extraction of heteroatomic classes based on acidity or basicity are typically necessary.[7,10] Vacuum distillation residue compositional analysis via GC/MS requires the separation of asphaltenes and maltenes (oleo-resins). Asphaltenes are heptane-insoluble molecules of wide-ranging polarity and molecular weight. Precipitation depends on solvent, solvent volume, and temperature. Moreover, maltenes (paraffinic, naphthenic, and −NSO polyaromatic hydrocarbons) must be separated into homologous fractions by adsorption, coagulation, and extraction prior to GC/MS analysis.[7] Such lengthy chromatographic pretreatment may introduce significant errors and systematic artifacts.[11]

Crude oil distillation isolates saturated and aromatic hydrocarbons by boiling point into products such as diesel, naphtha, kerosene, etc. Furthermore, crude oil distillation concentrates corrosive heteroatomic compounds in select distillation cuts. For example, light-end distillates are typically highly corrosive.[12] The total acid number (TAN), i.e., the grams of potassium hydroxide required to neutralize 1 g of oil, of a crude oil might be expected to correlate with the corrosivity of the oil. However, the TAN does not correlate directly with corrosivity. Rather, the concentration of specific classes (i.e., carboxylic acids, alkyl phenols, and nonpolar sulfur compounds) may contribute to corrosivity.[13−16]

Mass measurement alone cannot distinguish isomers of the same elemental composition and thus cannot generally define a unique molecular structure. However, ultrahigh-resolution Fourier transform−ion cyclotron resonance mass spectroscopy (FT−ICR MS) can definitively determine molecular elemental composition, by revealing the heteroatomic class degree of aromaticity, which leads to suggested possible molecular structures for eventual correlation with corrosivity. Electrospray ionization (ESI) FT−ICR MS is a proven method to achieve simultaneous, rapid, reproducible class-sorted molecular compositions for the thousands of unique species in fuel samples. ESI selectively generates $(M+H)^+$ or $(M-H)^-$ quasimolecular ions at atmospheric pressure via protonation or deprotonation without fragmentation. Therefore, ESI is best-suited to ionize the acidic/basic polar heteroatomic compounds that can cause problems in distillation. In addition, the unprecedented mass accuracy and resolution afforded by FT−ICR MS[17] allow for the resolution and assignment of >11 000 compositionally distinct compounds at a mass accuracy of <0.3 ppm in a single mass spectrum.[18] ESI FT−ICR MS[19,20] eliminates lengthy and problematic prior wet chemical separations and yields comprehensive type, class, molecular weight, and alkylation distributions. A molecular heteroatomic class composition distribution profile is the first step to adjust current upgrade methods to remove heteroatomic compounds of interest. Here, we apply negative-ion ESI FT−ICR MS to acidic polar −NSO species from low (563−606 °F), medium (606−853 °F), and high (853−1009 °F) distillates from a VGO in an effort to characterize molecular weight, type, and class distribution of polar acidic heteroatomic species.

Experimental Section

I. Samples. Light (295−319 °C, 563−606 °F), middle (319−456 °C, 606−853 °F), and heavy (456−543 °C, 853−1009 °F) distillates of a VGO were provided by ExxonMobil Research and Engineering (Annandale, NJ). The high-TAN VGO is moderate in regard to nitrogen-containing species and low in regard to sulfur-containing species. The high-TAN value allows us to investigate corrosivity contributions from specific acidic classes concentrated in the selected distillation cuts.

II. Sample Preparation for ESI FT−ICR MS. Sample preparation for the analysis of petroleum products by negative-ion ESI FT-ICR MS has been reported previously.[18] In summary, samples for analysis were diluted to 1 mg/mL in standard ESI spray mix for hydrocarbon analysis (50:50 toluene:MeOH). A 1-mL aliquot of each sample was reserved for analysis and spiked with 10 μL of 28% NH_4OH or glacial acetic acid, to facilitate the protonation/deprotonation of basic/acidic species in each sample. Each sample was delivered to the ionization source via a syringe pump at a rate of 400 nL/min through a 50 μm inner diameter (ID) fused-silica micro ESI needle under typical ESI conditions (2.1 kV; tube lens, 350 V; and heated capillary current, 3 A).[20]

III. Mass Analysis. Each distillation cut was analyzed with a home-built 9.4-T 22-cm horizontal room-temperature bore diameter (Oxford Corp., Oxford Mead, UK) FT−ICR mass spectrometer at the National High Magnetic Field Laboratory.[21] A modular ICR data acquisition system (MIDAS) was used to collect and process ICR data.[22,23] Calibrant ions were generated by an electrospray of Agilent (Palo Alto, CA) HP mix. Ions were accumulated externally in a linear octopole ion trap for 30 s and transferred through rf-only multipoles to a 10-cm-diameter, 30-cm-long open cylindrical Penning ion trap.[24] Octapole ion guides were operated at 1.7 MHz

(10) Snyder, L. R.; Buell, B. E. Nitrogen and Oxygen Compound Types in Petroleum. A General Separation Scheme. *Anal. Chem.* **1968**, *40* (8), 1295−1302.

(11) Galimberti, R.; Ghiselli, C.; Chiaramonte, M. A. Acidic polar compounds in petroleum: a new analytical methodology and applications as molecular migration indices. *Org. Geochem.* **2000**, *31* (12), 1375−1386.

(12) Laredo, G. C.; Lopez, C. R.; Alvarez, R. E.; Cano, J. L. Naphthenic acids, total acid number and sulfur content profile characterization in Isthmus and Maya crude oils. *Fuel* **2004**, *83* (11−12), 1689−1695.

(13) Ioppolo, M.; Alexander, R.; Kagi, R. I. Identification and Analysis of C0−C3 Phenols in Some Australian Crude Oils. *Org. Geochem.* **1992**, *18* (5), 603−609.

(14) Meredith, W.; Kelland, S. J.; Jones, D. M. Influence of biodegradation on crude oil acidity and carboxylic acid composition. *Org. Geochem.* **2000**, *31* (11), 1059−1073.

(15) Slavcheva, E.; Shone, B.; Turnbull, A. Review of naphthenic acid corrosion in oil refining. *Br. Corros. J.* **1999**, *34* (2), 125−131.

(16) Turnbull, A.; Slavcheva, E.; Shone, B. Factors controlling naphthenic acid corrosion. *Corrosion* **1998**, *54* (11), 922−930.

(17) Marshall, A. G.; Hendrickson, C. L.; Jackson, G. S. Fourier transform ion cyclotron resonance mass spectrometry: A primer. *Mass Spectrom. Rev.* **1998**, *17* (1), 1−35.

(18) Hughey, C. A.; Rodgers, R. P.; Marshall, A. G. Resolution of 11 000 compositionally distinct components in a single electrospray ionization Fourier transform ion cyclotron resonance mass spectrum of crude oil. *Anal. Chem.* **2002**, *74* (16), 4145−4149.

(19) Zhan, D. L.; Fenn, J. B. Electrospray mass spectrometry of fossil fuels. *Int. J. Mass Spectrom.* **2000**, *194* (2−3), 197−208.

(20) Emmett, M. R.; White, F. M.; Hendrickson, C. L.; Shi, S. D. H.; Marshall, A. G. Application of micro-electrospray liquid chromatography techniques to FT-ICR MS to enable high-sensitivity biological analysis. *J. Am. Soc. Mass Spectrom.* **1998**, *9* (4), 333−340.

(21) Senko, M. W.; Hendrickson, C. L.; Pasa-Tolic, L.; Marto, J. A.; White, F. M.; Guan, S.; Marshall, A. G. Electrospray Ionization FT−ICR Mass Spectrometry at 9.4 T. *Rapid Commun. Mass Spectrom.* **1996**, *10*, 1824−1828.

(22) Blakney, G. T.; van der Rest, G.; Johnson, J. R.; Freitas, M. A.; Drader, J. J.; Shi, S. D.-H.; Hendrickson, C. L.; Kelleher, N. L.; Marshall, A. G. Further Improvements to the MIDAS Data Station for FT−ICR Mass Spectroscopy. In *Proceedings of the 49th ASMS Conference on Mass Spectrometry, and Allied Topics*, Chicago, IL, 2001.

(23) Senko, M. W.; Canterbury, J. D.; Guan, S.; Marshall, A. G. A High-Performance Modular Data System for FT-ICR Mass Spectrometry. *Rapid Commun. Mass Spectrom.* **1996**, *10*, 1839−1844.

(24) Senko, M. W.; Hendrickson, C. L.; Emmett, M. R.; Shi, S. D.-H.; Marshall, A. G. External accumulation of ions for enhanced electrospray ionization Fourier transform ion cyclotron resonance mass spectrometry. *J. Am. Soc. Mass Spectrom.* **1997**, *8* (9), 970−976.

with 100 V_{p-p} rf amplitude and a 900 μs transfer period.[25] Slightly different conditions were used for the light distillation cut, to optimize transmission of lower-mass ions: ion guides were operated at 2.0 MHz and a 700 μs transfer period. Broadband frequency-sweep (chirp) dipolar excitation (~70 kHz to 641 kHz at a sweep rate of 150 Hz/μs and a peak-to-peak amplitude of 190 V) was followed by direct-mode image current detection to yield 4 Mword time-domain data. Two hundred fifty time-domain data sets were co-added and Hanning apodized, followed by a single zero-fill before fast Fourier transformation and magnitude calculation. Frequency was converted to mass-to-charge ratio by the quadrupolar electric potential approximation.[26,27] Infrared multiphoton dissociation (IRMPD) experiments were performed with a Synrad (Model 48-2, Mukilteo, WA) 40 W continuous-wave CO_2 laser (λ = 10 μm) for 100−450 ms.

IV. Mass Calibration. Mass spectra were frequency-to-*m*/*z* calibrated externally, with respect to an Agilent No. G2421A electrospray "tuning mix", for all peaks with a magnitude of three standard deviations above the baseline noise. Externally calibrated spectra were then internally recalibrated with respect to the most abundant homologous alkylation series for each sample. All masses were then converted to the Kendrick mass scale.[28] Kendrick-sorted masses were imported into Microsoft Excel for identification with a formula calculator, as previously reported.[29] In summary, molecular formulas were assigned to peaks of lowest *m*/*z* value for each Kendrick Mass Defect (KMD) series. Peaks of higher *m*/*z* ratio for the same KMD value were assigned by adding multiples of CH_2 to the molecular formula. Calculations were limited to formulas containing less than 100 ^{12}C, 2 ^{13}C, 200 ^{1}H, 5 ^{14}N, 10 ^{16}O, 3 ^{32}S, and 1 ^{34}S. If more than one possible formula was generated for a specific mass, one or more could almost always be confirmed or eliminated by the presence/absence of a corresponding ^{13}C, ^{18}O, or ^{34}S peak. All observed species were singly charged, as evidenced by the unit *m*/*z* separation between mass spectral peaks corresponding to the $^{12}C_c$ and $^{13}C^{12}C_{c-1}$ isotopic variants for each elemental composition.

Results and Discussion

I. Mass Distribution. Figure 1 shows negative-ion ESI FT−ICR high-resolution mass spectra (average $m/\Delta m_{50\%}$ > 360 000, in which $\Delta m_{50\%}$ is the mass spectral peak full width at half-maximum (FWHM) peak height) of the acidic components from three temperature-range distillates of a VGO. Figure 2 shows positive-ion ESI FT−ICR mass spectra of the basic components of the same distillates. The light distillates shown in Figures 1 and 2 were collected after CO_2 laser infrared multiphoton dissociation (IRMPD). The *m*/*z* distributions for the light, middle, and heavy distillates are analogous to those previously reported.[4,30] Light VGO acidic and basic distillate constituents ranged from 200 to 300 Da, acidic and basic middle distillates ranged from 300 to 650 Da, acidic heavy distillates ranged from 300 to 650 Da, and basic heavy distillates ranged from 300 to 750 Da. Basic components are more varied than acidic components: 559, 720, and 1183 acidic species resolved in the light, middle, and heavy distillates, compared to 203, 2404, and 2875 basic species in the light, middle, and heavy distillates. The higher spectral complexity at higher distillation cut temperatures is confirmed in the literature.[4,30−32]

We now proceed to analyze distillation cuts in terms of heteroatom class, double bond equivalents (DBE), and extent of alkylation.[32,33] DBE is the number of rings plus double bonds and may be determined from the elemental composition:[34]

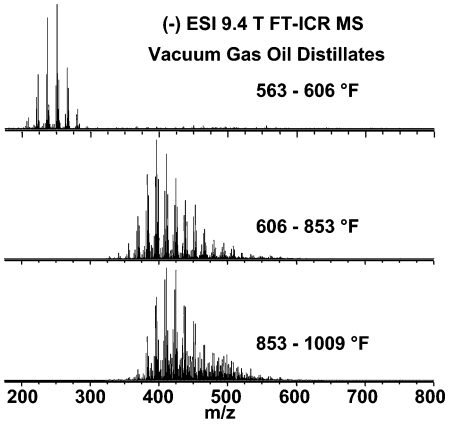

Figure 1. Broadband negative-ion electrospray ionization (ESI) 9.4-T Fourier transform−ion cyclotron resonance (FT-ICR) mass spectra of a vacuum gas oil (VGO) at three distinct stages of distillation. Note the increase in complexity and shift to higher *m*/*z* with increasing distillation temperature. IRMPD was used to dissociate multimers to produce the top spectrum (see below).

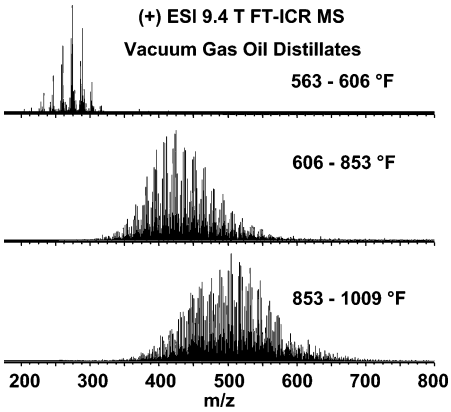

Figure 2. Broadband positive-ion ESI 9.4 T FT−ICR mass spectra of a VGO at three distinct stages of distillation. Note the increase in complexity and shift to higher *m*/*z* with increasing distillation temperature. IRMPD was used to dissociate multimers to produce the top spectrum (see below).

(25) Hendrickson, C. L.; Quinn, J. P.; Emmett, M. R.; Marshall, A. G. Quadrupole Mass Filtered External Accumulation for Fourier Transform Ion Cyclotron Resonance Mass Spectrometry. In *Proceedings of the 48th ASMS Conference on Mass Spectrometry and Allied Topics*, Long Beach, CA, 2000.

(26) Ledford, E. B.; Rempel, D. L.; Gross, M. L. Space-Charge Effects in Fourier Transform Mass-Spectrometry. 1. Electrons. *Int. J. Mass Spectrom., Ion Process.* **1984**, 55 (2), 143−154.

(27) Shi, S. D.-H.; Drader, J. J.; Freitas, M. A.; Hendrickson, C. L.; Marshall, A. G. Comparison and interconversion of the two most common frequency-to-mass calibration functions for Fourier transform ion cyclotron resonance mass spectrometry. *Int. J. Mass Spectrom.* **2000**, *196*, 591−598.

(28) Kendrick, E. A Mass Scale Based on CH_2 = 14.0000 for High-Resolution Mass Spectrometry of Organic Compounds. *Anal. Chem.* **1963**, *35* (13), 2146−2154.

(29) Hughey, C. A.; Hendrickson, C. L.; Rodgers, R. P.; Marshall, A. G.; Qian, K. N. Kendrick mass defect spectrum: A compact visual analysis for ultrahigh-resolution broadband mass spectra. *Anal. Chem.* **2001**, *73* (19), 4676−4681.

(30) Snyder, L. R. Nitrogen and Oxygen Compound Types in Petroleum. Total Analysis of a 400−700 °F Distillate from a California Crude Oil. *Anal. Chem.* **1969**, *41* (2), 314−323.

(31) Roussis, S. G.; Prouix, R., The characterization of basic petroleum extracts by high-resolution mass spectrometry and simultaneous orthogonal acceleration time-of-flight-magnet scanning tandem mass spectrometry. *Energy Fuels* **2004**, *18* (3), 685−697.

(32) Al-Zaid, K.; Khan, Z. H.; Hauser, A.; Al-Rabiah, H. Composition of high boiling petroleum distillates of Kuwait crude oils. *Fuel* **1998**, *77* (5), 453−458.

(33) Briker, Y.; Ring, Z.; Iacchelli, A.; McLean, N. Miniaturized method for separation and quantification of nitrogen species in petroleum distillates. *Fuel* **2003**, *82* (13), 1621−1631.

(34) Pellegrin, V. Molecular Formulas of Organic-Compounds−The Nitrogen Rule and Degree of Unsaturation. *J. Chem. Educ.* **1983**, *60* (8), 626−633.

$$\mathrm{DBE} = c - \frac{1}{2}h + \frac{1}{2}n + 1 \quad \text{(for the neutral molecule, } C_cH_hN_nO_oS_s\text{)} \quad (1)$$

The increase in spectral complexity with increasing distillation temperature is not due solely to more heteratomic classes.[4,10,30,35] A given heteratomic class may distill over a narrow temperature range, but another could span a range of distillation cuts. Acidic and basic NSO compound distillation cut segregation at the selected temperature ranges may be further analyzed by heteroatom class distribution, carbon number versus DBE for a given class, and van Krevelen plots.

II. Heteroatom Classes. Acidic and basic NSO heteratomic class compositions for each distillation unit of the VGO are shown in Figures 3 and 4, respectively. Note that abundances are scaled relative to the highest-magnitude peak in each mass spectrum, so that even if the *absolute* abundance of a given class is the same for two samples, its *relative* abundance will depend on differences in the abundances of other species. Nevertheless, some trends are clear. For example, if compounds of a given class maintain the same DBE and alkylation values across different distillate fractions, then any change in their relative abundance presumably reflects a corresponding change in the absolute abundance(s) of other species. For example, of the acidic classes present at >1% relative abundance (O, O_2, O_3S, O_4S, N, and NO) (see Figure 3), oxygenated species (mostly O_2) dominate the light distillates, nitrogen-containing species become increasingly prevalent in the heavy distillates, and sulfur-containing classes drop out with increasing distillation temperature. The negative-ion ESI spectrum of the light distillates is dominated by acidic oxygenated species and is completely devoid of pyrrolic (acid-nitrogenated) species.

Negative-ion O_2-class ions present at >60% relative abundance are a focal point of each distillate fraction (see Figure 3). O_2-class ions in the negative-ion mass spectra are presumably carboxylic acids. The selective ionization of carboxylic acids by negative-ion ESI has been reported previously.[36,37] Acidic O_2-class compounds distill across a broad temperature range, whereas the acidic O, O_3S, O_4S, and N classes distill over narrow ranges. Although sulfur-containing acids are implicated in corrosion during high-temperature distillation, we have detected sulfur-containing acids only in the light and middle distillates. Acidic NO species appear only in the heavy distillation cut sample, and only at low relative abundance.

Of the basic species in the positive-ion mass spectra (N, N_2, NO, NO_2, NS, O_2, O_4, and OS) (see Figure 4), pyridinic nitrogen-containing compounds (N-class) constitute ~60% of the total for all three distillates. Of the remaining species, only the OS class is present at significant abundance, and then only in the lightest distillate. ESI FT−ICR mass spectra of model RSR OS compounds reflect the DBE distribution of OS ions detected by previous positive-ion ESI FT−ICR experiments with

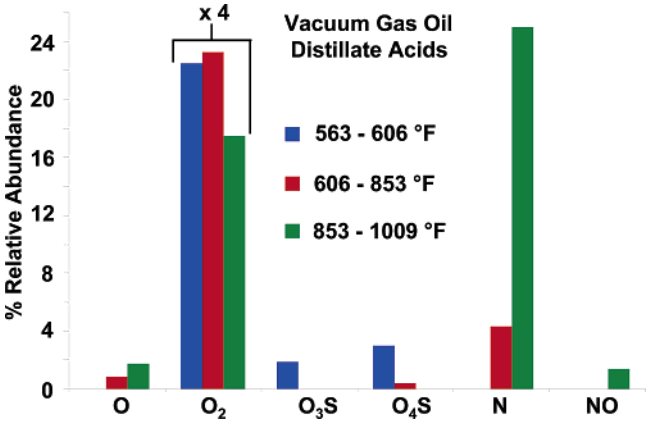

Figure 3. Relative abundances of acidic compound classes of >1% relative abundance in a vacuum gas oil at three separate stages of distillation. The O_2 class is dominant (>60% relative abundance) in each distillation cut. Nitrogen-containing species are observed in the heavier distillates, whereas sulfur-containing species are observed only in the lighter distillates.

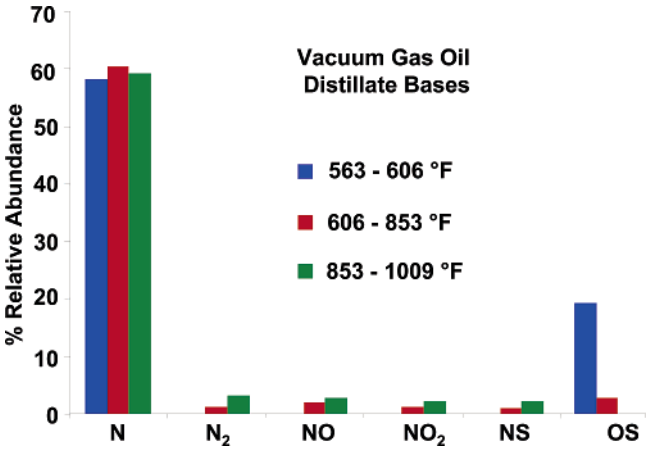

Figure 4. Relative abundances of basic compound classes of >1% relative abundance in a vacuum gas oil at three separate stages of distillation. Nitrogen-containing species dominate in all of the distillate fractions.

diesel fuels[38] and OS ions detected in this paper. Finally, as for the acidic species, oxygen/sulfur-containing species from positive-ion electrospray are exclusive to the light and middle distillates. Variation of heteroatomic species class among the distillation cut samples also depends on aromaticity (see below).

III. Oxygen-Containing Species. Acidic oxygenated species are major components in each distillation cut sample. To further probe their structures, we now focus on individual classes, with respect to DBE and carbon number. A van Krevelen plot presents a concise graphical display to track changes in heteroatomic class, type, and extent of alkylation. For example, Figure 5 plots isoabundance contours for the hydrogen/carbon (H/C) ratio versus the oxygen/carbon (O/C) ratio for each elemental composition that contains at least one O atom. Thus, the O/C ratio separates compositions horizontally by compound class (O, O_2, O_3, etc.). Elemental compositions shift vertically downward with increasing DBE (i.e., increasing aromaticity).

(35) Snyder, L. R.; Buell, B. E.; Howard, H. E. Nitrogen and Oxygen Compound Types in Petroleum. Total Analysis of a 700−850 °F Distillate from a California Crude Oil. *Anal. Chem.* **1968**, *40* (8), 1303−1317.

(36) Hsu, C. S.; Dechert, G. J.; Robbins, W. K.; Fukuda, E. K. Naphthenic acids in crude oils characterized by mass spectrometry. *Energy Fuels* **2000**, *14* (1), 217−223.

(37) Qian, K. N.; Robbins, W. K.; Hughey, C. A.; Cooper, H. J.; Rodgers, R. P.; Marshall, A. G. Resolution and identification of elemental compositions for more than 3000 crude acids in heavy petroleum by negative-ion microelectrospray high-field Fourier transform ion cyclotron resonance mass spectrometry. *Energy Fuels* **2001**, *15* (6), 1505−1511.

(38) Hughey, C. A.; Hendrickson, C. L.; Rodgers, R. P.; Marshall, A. G. Elemental composition analysis of processed and unprocessed diesel fuel by electrospray ionization Fourier transform ion cyclotron resonance mass spectrometry. *Energy Fuels* **2001**, *15* (5), 1186−1193.

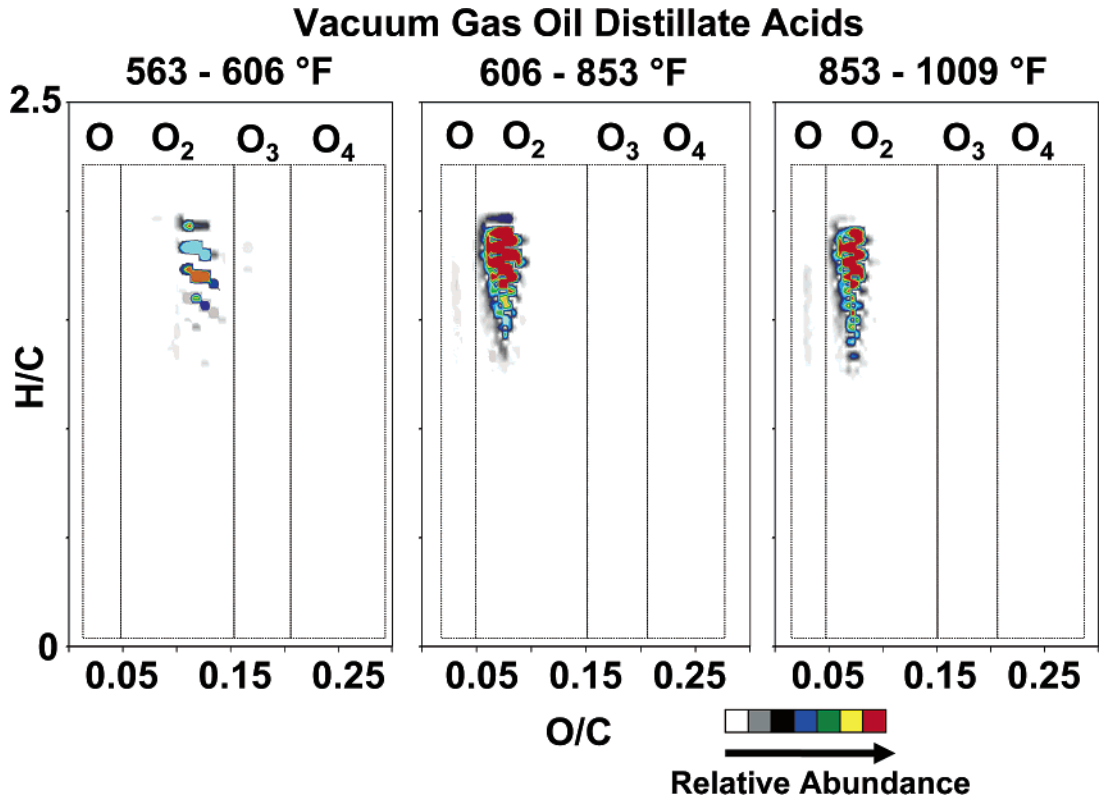

Figure 5. Three-dimensional (3D) van Krevelen diagram of oxygen-containing negative ions from light, middle, and heavy distillates of the VGO.

Finally, compositions with a given DBE value separate diagonally as a function of alkyl chain length.[39]

III.A. O Class. O-class compounds that are common to the middle and heavy distillates of crude oil include aldehydes, phenols, furans, and ketones.[4,10,30,35] However negative-ion ESI efficiency is low for aldehydes, furans, and ketones. ESI FT−ICR MS selectively ionizes phenolic species in petroleum.[18] O-class compounds are completely absent from ESI FT−ICR MS of the light distillates and are present only at DBE > 4 (hence, aromatics rather than alkenes with four double bonds or an alcohol with four saturated rings) in the middle and heavy distillates (see Figure 5). Phenol and polycyclic or polyaromatic phenolic species exhibit DBE values that are ≥4, consistent with the lowest DBE range for O-class ions from the three distillation cuts (see Figure 6, in which DBE is plotted as a function of carbon number for species only from the O class).

Figure 6 shows that the phenolic O-class species share a narrow carbon number distribution ($C_{27}-C_{38}$ and $C_{27}-C_{39}$ for the middle and heavy distillation cuts, respectively) but a relatively wide DBE value distribution. Carbon number and DBE distributions of the phenolics remain constant (and therefore presumably represent similar compounds) as the distillation temperature increases. Prior analysis of the distribution of aromatic mono-oxygen species from a Californian crude oil by Snyder reported phenols in middle distillates with 4 < DBE < 11, with the most abundant at DBE = 5; Snyder also reported that phenolics were present in heavy distillates at 4 < DBE < 15 and were most abundant at DBE = 5 and 6.[4,10,30,35] Despite low ESI efficiency for the O class, our results reflect similar trends, but without >27 steps for fractionation prior to detection.

III.B. O_2 Class. O_2-class negative ions are the most abundant O_x ions in each distillate fraction (see Figures 3 and 5). The slight O/C shift for the middle and heavy distillates is attributed to higher carbon numbers and subsequently higher degree of alkylation of heavier distillates. Light distillate acidic O_2 species are low in molecular weight and low in aromaticity (Figure 7). O_2-class DBE values increase somewhat (and are found at higher average mass) in the middle and heavy distillates, but DBE = 3 (presumably nonaromatic dicyclic) O_2 species dominate in all distillation cuts (with increasing alkylation at higher distillation temperature). Thus, *carboxylic acids fractionate by alkyl chain length, but not by DBE value*. $C_{21}-C_{43}$ naphthenic, monoaromatic, diaromatic, and triaromatic O_2 species populate the middle and heavy distillates. It is unlikely that species of the higher DBE range are polycyclics, because previous work has shown that series that start at a high carbon number and DBE are aromatics and polyaromatics.[36] O_2 species from the middle and heavy distillates of earlier publications are aliphatic.[4,10,30,35] However, we demonstrate not only aliphatic forms of O_2 species at DBE = 1 (the double bond is from the carbonyl) but also aromatic and polyaromatic forms at DBE = 5−14. Acyclic, polycyclic, and polyaromatic carboxylic acids are classified as naphthenic acids.[40]

Low-molecular-weight naphthenic acids that distill at 220−440 °C (428−752 °F) are corrosive.[12] Reports indictate an initial spike in corrosivity in VGO distillation at ∼300 °C.[12] O_2 species detected in the light distillates fall within the aforementioned temperature, DBE, and molecular-weight ranges and therefore qualify as corrosive and pose a threat to fuel storage stability. Middle distillate O_2-class species distill within the temperature and DBE range for corrosive acids.

(39) Kim, S.; Kramer, R. W.; Hatcher, P. G. Graphical method for analysis of ultrahigh-resolution broadband mass spectra of natural organic matter, the van Krevelen diagram. *Anal. Chem.* **2003**, *75* (20), 5336−5344.

(40) Rogers, V. V.; Liber, K.; MacKinnon, M. D. Isolation and characterization of naphthenic acids from Athabasca oil sands tailings pond water. *Chemosphere* **2002**, *48* (5), 519−527.

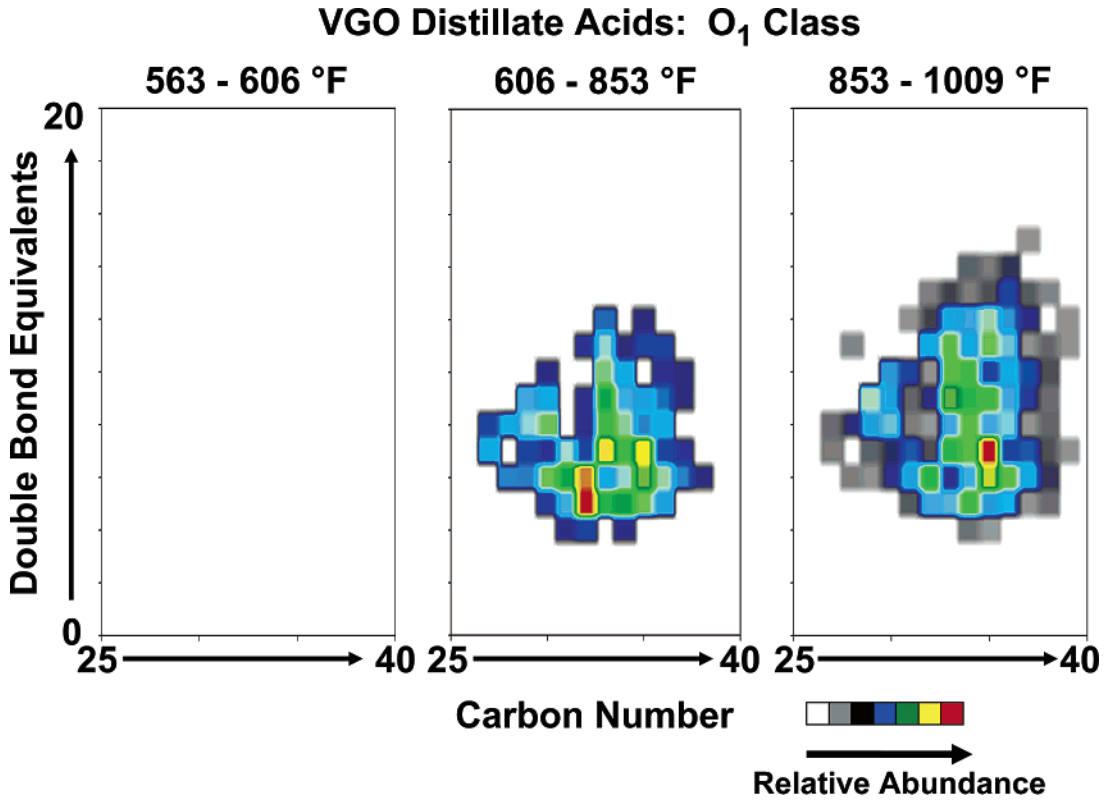

Figure 6. Three-dimensional (3D) double bond equivalents (DBE) versus carbon number distribution for O_1-class compounds for each distillation cut unit from a VGO.

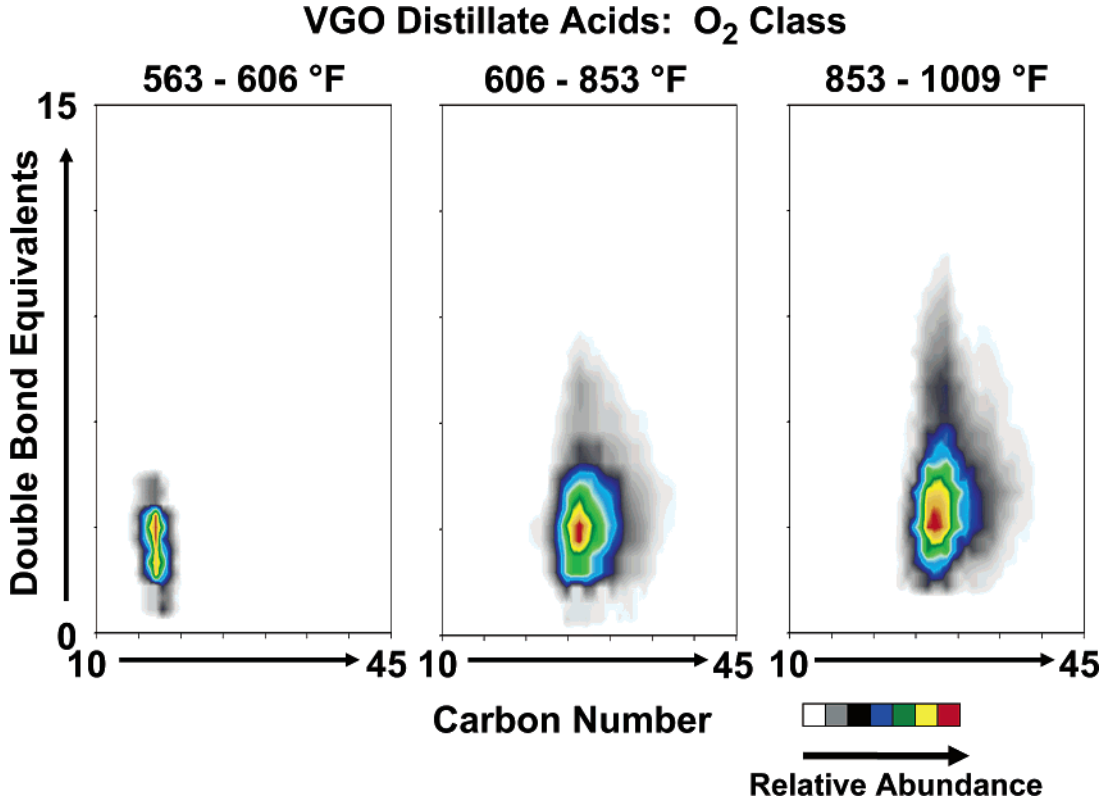

Figure 7. Three-dimensional (3D) DBE versus carbon number distribution for O_2-class compounds for each distillation cut unit from a VGO.

IV. Noncovalent Multimers. Low-molecular-weight carboxylic acids may form supramolecular oligomers such as noncovalent dimers and trimers. The possibility for self-associating molecules to form oligomeric solution-phase clusters that survive in the gas phase may be established by the use of IRMPD, a noncoherent multiphoton absorption process that heats a gas-phase ion until the weakest (covalent or noncovalent) bond breaks.[41,42] The negative-ion ESI FT−ICR mass spectrum of the light distillates without IRMPD (Figure 8, top) shows

(41) Woodlin, R. L.; Bomse, D. S.; Beauchamp, J. L. Multiphoton Dissociation of Molecules with Low Power Continuous Wave Infrared Laser Radiation. *J. Am. Chem. Soc.* **1978**, *100*, 3248−3250.

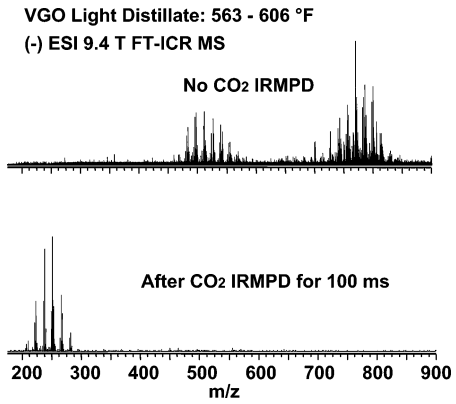

Figure 8. Broadband negative-ion ESI 9.4-T FT−ICR MS spectra of VGO light distillates without infrared irradiation (top) and with infrared irradiation (bottom), confirming that higher *m*/*z* species are noncovalent dimers and trimers of lower *m*/*z* species.

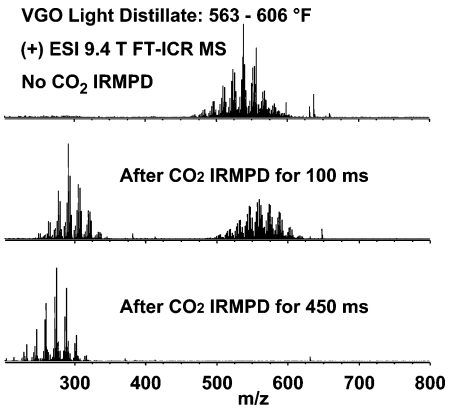

Figure 9. Broadband positive-ion ESI 9.4-T FT−ICR mass spectra of VGO light distillates without infrared irradiation (top), and with infrared irradiation (middle, bottom), confirming partial dissociation of dimers (middle) and complete dissociation of dimers (bottom).

broad humps of peaks separated by ∼250 Da. Low-molecular-weight carboxylic acids are known to form supramolecular oligomeric structures in solution and low-polarity solvents via strong intermolecular OH−O hydrogen bonds.[43−46] Low-power CO_2 laser IRMPD suffices to dissociate carboxylic acid noncovalent oligomers in the ICR cell without breaking covalent bonds, to leave monomeric ions.[47] The bottom portion of Figure 8 shows the broadband mass spectrum of the light distillate ions after 100 ms of infrared irradiation. The multimer distributions clearly dissociate to leave monomers of 200−300 Da (see Figure 8 (bottom) and Figure 1 (top)). IRMPD at similar laser power did *not* affect the molecular-weight distributions in ESI FT−ICR mass spectra of the middle and heavy distillates, which therefore do not appear to form noncovalent multimers.

V. Nitrogen-Containing Species. We observe pyrrolic (acidic) nitrogen-containing (N-class) compounds in the medium and heavy distillates, and pyridinic (basic) nitrogen-containing (N-class) compounds in each distillate (see Figures 3 and 4). As for the basic species observed by positive-ion ESI, low-power infrared irradiation for 100 ms dissociates noncovalent dimers to leave monomers at 200−325 Da (see Figure 9 (top, middle)). Partial dissociation after 100 ms irradiation becomes complete after 450 ms (see Figure 9 (bottom) and Figure 2 (top)). Moreover, in regard to the acidic components, the middle and heavy distillate N-class ions were unaffected by infrared irradiation and thus presumably do not aggregate to form multimers. Figure 10 shows DBE versus carbon number distributions for basic N-class compounds (from positive-ion ESI FT-ICR mass spectra) for each distillation cut. The average DBE value increases from 5 to 7 to 9, and the average carbon number increases from 18 to 30 to 37 in proceeding from low to middle to high distillation temperatures, corresponding to increased aromaticity and alkylation with increasing distillation temperature.

Acidic nitrogenated hydrocarbons become more important as we shift focus to the middle and heavy distillates.[33] The hydrotreatment catalytic surface can be poisoned by nonbasic nitrogenated species in middle distillates.[48] In contrast to the basic nitrogen classes (N, N_2, NO, NO_2, and NS) detected by positive-ion ESI, the acidic nitrogen species observed by negative-ion ESI are limited to N and NO classes. Alkyl carbazoles belonging to the N class (i.e., observed by negative-ion ESI) are the most abundant of all nitrogenated species, consistent with prior literature.[10,33,35]

As noted previously, the light distillation cut is devoid of pyrrolic species. Previous reports describe nitrogenated species concentrated in distillates at temperatures of >400 °C (752 °F),[31] i.e., well above the lowest distillation temperature in our samples, but consistent with our results for the middle distillates. Here, acidic N-class compounds exhibit similar DBE and carbon number ranges for both the middle and heavy distillates (Figure 11), with some shift to higher values of both parameters at higher distillation temperature, consistent with higher molecular weights at higher distillation temperature. Our DBE range for negative-ion N species is consistent with prior analyses of a California crude oil.[4,10,30,35]

The acidic NO class is observed exclusively in the heavy distillate, at much lower abundance than the N class (see Figure 4), consistent with previous literature.[4,10,30,35] The NO class is observed in the heavy distillate (see Figure 12), at DBE = 8−17 and in the carbon number range of C_{28}−C_{38}. Species of the NO class in the heavy distillation cut span a higher DBE range than those of the N class; thus, the NO class is more extensively aromatic than the N class. However, N-class compounds have more-extensive alkylation than those of the NO class, as reflected by the carbon number distributions in Figures 11 and 12.

VI. Sulfur-Containing Species. Although present in relatively low abundance in bulk oils, O_xS species are efficiently ionized by electrospray and therefore readily observed in the

(42) Little, D. P.; Speir, J. P.; Senko, M. W.; O'Connor, P. B.; McLafferty, F. W. Infrared Multiphoton Dissociation of Large Multiply-Charged Ions for Biomolecule Sequencing. *Anal. Chem.* **1994**, *66*, 2809−2815.

(43) Schaper, K. J.; Kunz, B.; Raevsky, O. A. Analysis of water solubility data on the basis of HYBOT descriptors. Part 2. Solubility of liquid chemicals and drugs. *QSAR Comb. Sci.* **2004**, *22* (9−10), 943−958.

(44) Infantes, L.; Mahon, M. F.; Male, L.; Raithby, P. R.; Teat, S. L.; Sauer, J.; Jagerovic, N.; Elguero, J.; Motherwell, S. 1,2,4,5-Tetrazines vs. carboxylic acid dimers: Molecular chemistry vs. supramolecular chemistry. *Helv. Chim. Acta* **2003**, *86* (4), 1205−1221.

(45) Vawdrey, A. C.; Oscarson, J. L.; Rowley, R. L.; Wilding, W. V. Vapor-phase association of n-aliphatic carboxylic acids. *Fluid Phase Equilib.* **2004**, *222*, 239−245.

(46) Goodman, D. S. The Distribution of Fatty Acids between Normal-Heptane and Aqueous Phosphate Buffer. *J. Am. Chem. Soc.* **1958**, *80* (15), 3887−3892.

(47) Rodgers, R. P.; Hendrickson, C. L.; Emmett, M. R.; Marshall, A. G.; Greaney, M.; Qian, K. N. Molecular characterization of petroporphyrins in crude oil by electrospray ionization Fourier transform ion cyclotron resonance mass spectrometry. *Can. J. Chem.* **2001**, *79* (5), 546−551.

(48) Wandas, R.; Chrapek, T. Hydrotreating of middle distillates from destructive petroleum processing over high-activity catalysts to reduce nitrogen and improve the quality. *Fuel Process. Technol.* **2004**, *85* (11), 1333−1343.

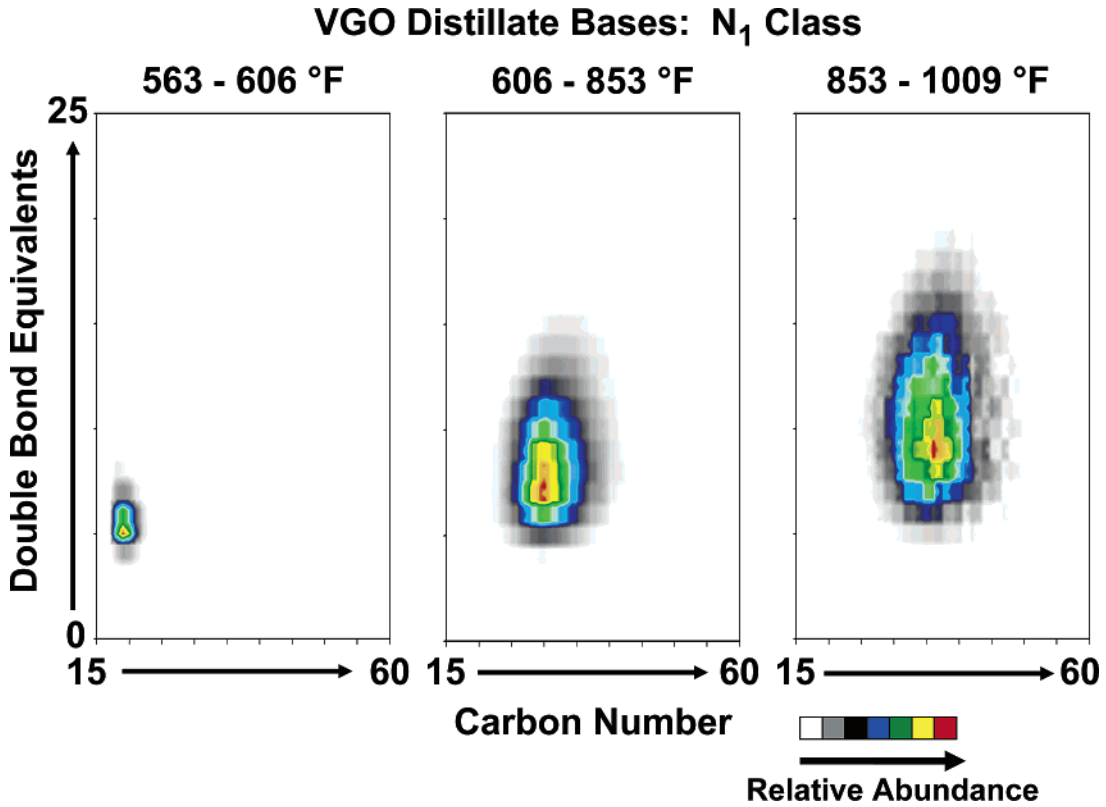

Figure 10. Three-dimensional (3D) DBE versus carbon number distribution for the positive-ion N_1-class compounds for each distillation cut from a VGO.

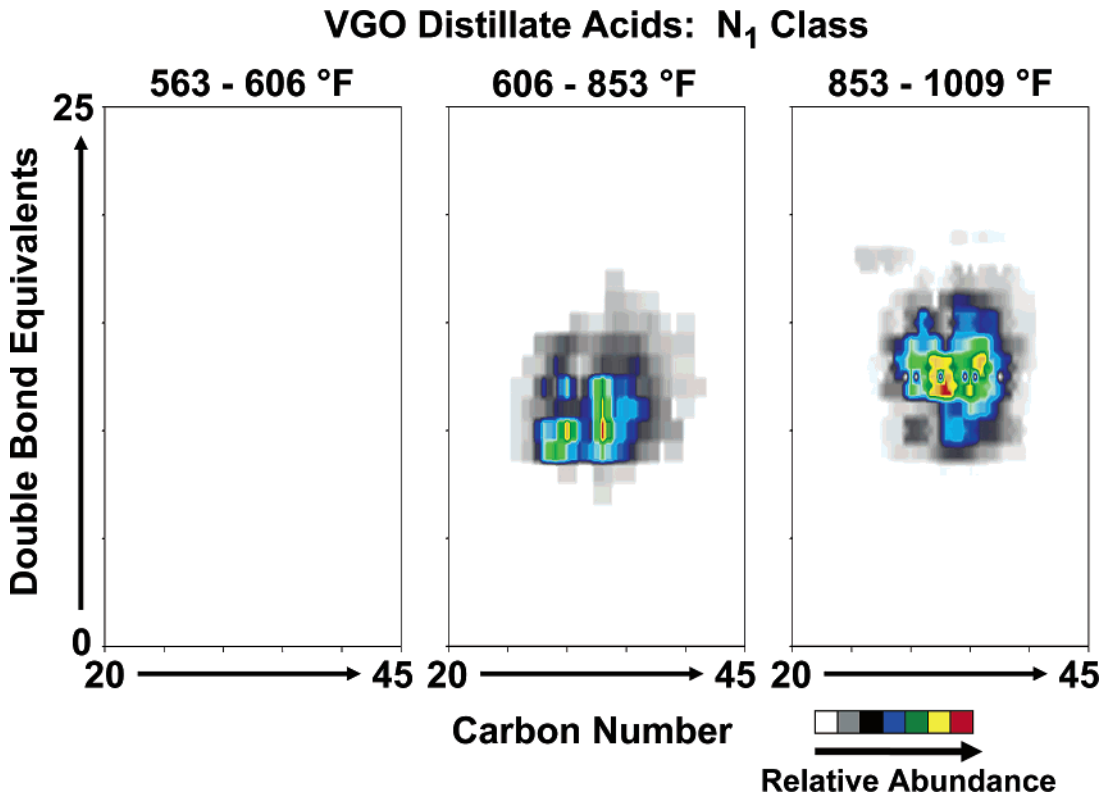

Figure 11. Three-dimensional (3D) DBE versus carbon number distribution for the negative-ion N_1-class compounds for the heavy distillates from a VGO.

VGO distillates. Acidic and basic O_xS are observed only in the light and middle distillates. Positive-ion O_xS ions have been detected in diesel fuel previously via FT−ICR MS.[38] Diesel and jet fuels distill at 400−630 °F.[49] All of the light distillates and only a fraction of the middle distillates fall within that range. Heavy distillates do not fall within that range and are devoid

(49) Algelt, K. H.; Boduszynski, M. M. *Composition and Analysis of Heavy Petroleum Fractions*; Marcel Dekker: New York, 1994; pp 44−50.

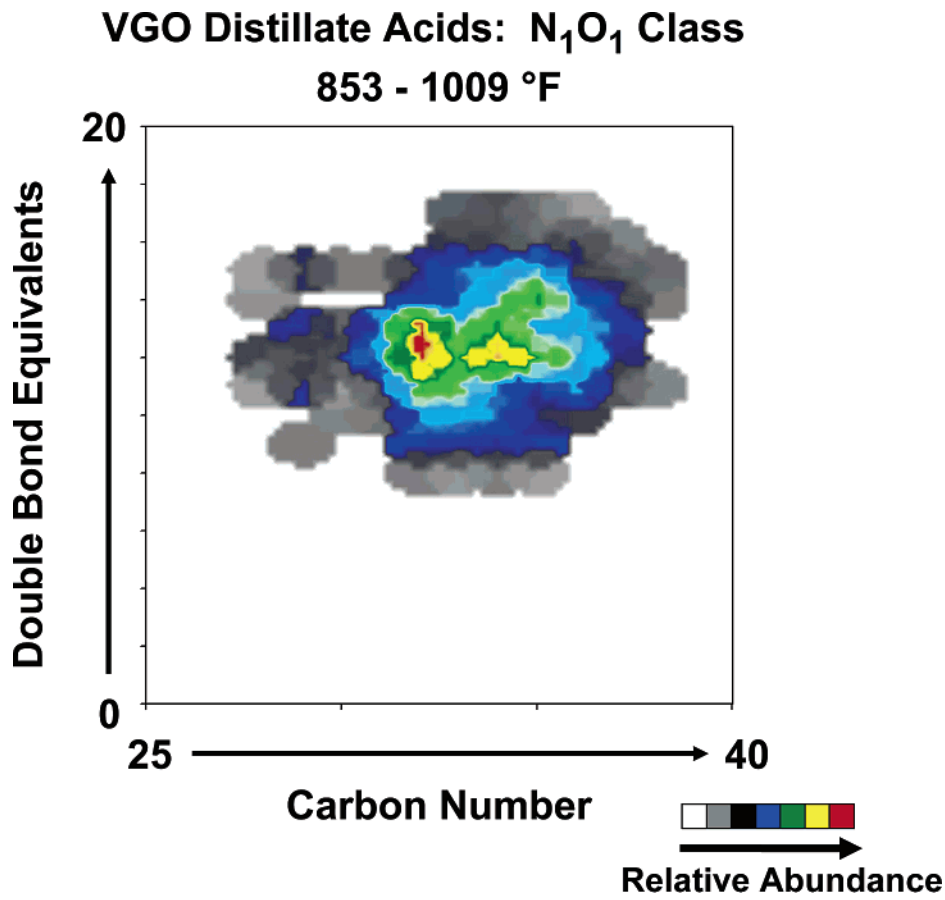

Figure 12. Three-dimensional (3D) DBE versus carbon number distribution for the heavy distillate negative-ion ESI N_1O_1-class compounds.

of O_xS species. Therefore, O_xS species are characteristic of lighter ends. Light and middle distillate acidic and basic O_xS species exhibit different abundances and class varieties. Acidic O_3S, O_4S, and basic OS were most abundant (see Figures 3 and 4). Acidic O_xS species are present primarily at low DBE and carbon number values that are indicative of acyclic, dicyclic, or monoaromatic compounds (Figure 13). Although both O_3S and O_4S are present at detectable abundance in the light distillate at DBE = 0−6, the O_3S class is most abundant at DBE = 4 and the O_4S class is most abundant at DBE = 0 in the light distillate. O_4S middle distillates are most abundant at DBE = 2 and 3. O_3S acyclic and monocyclic molecules are absent from the middle distillates, and the carbon number distribution of O_4S compounds increases dramatically as one proceeds from the light distillate (C_{12}−C_{15}) to the middle distillate (C_{20}−C_{32}). Detected basic OS compounds are predominantly sodiated adducts at >20% relative abundance in the light distillate (DBE = 1−6, C_{14}−C_{18}), and <5% (DBE = 1−9, C_{18}−C_{32}) in the middle distillate. The sodiated OS compounds detected by positive-ion ESI FT-ICR MS are most abundant at DBE = 3 in the light distillate and DBE = 4 in the middle distillate. As for the O_2 class (Figure 7), O_xS species fractionate via alkylation (Figure 13) and not via DBE from the light distillates to the middle distillates.

Oxygen-containing RSR compound reactions with H_2 or RSH compounds enhance naphthenic acid corrosion by producing water. Low-molecular-weight naphthenic acids are water-soluble and corrode iron surfaces after dissociation.[50] Segregation of O_xS species to the lighter ends of our VGO correlates with the high incidence of corrosivity at a temperature of 572 °F, as observed previously.[12] Although molecular structures of the light and middle distillate O_xS species (Figure 13) cannot be assigned based only on mass measurement, we can eliminate some possibilties based on DBE and ionization efficiency. For example, several O_xS species found in the VGO distillates generate DBE values of <4. O_xS compounds of DBE < 4 cannot be hydroxylated benzothiophenes for which DBE ≥ 6. O_xS species of DBE = 0 and 1 may be cyclic with a sulfate polar headgroup or polyhydroxylated sulfoxides. However, at DBE = 3−6, O_xS compounds could be thiophenes or benzothiophenes with carboxylic or hydroxyl aliphatic side chains. MS^n (tandem mass spectrometry) experiments (with model compounds, because there are too many elemental compositions of the same nominal mass in the VGO) would be needed to distinguish these possibilities.

Conclusion

Determination of compositional differences in a vacuum gas oil (VGO), as a function of distillation temperature, previously required more than 27 pretreatment steps to separate compounds, with respect to functional group and aromaticity for mass analysis. Such a lengthy benchtop pretreatment can introduce contamination as well as environmental concerns from the use and disposal of large quantities of organic solvents. However, electrospray ionization Fourier transform−ion cyclotron resonance mass spectrometry (ESI FT−ICR MS) can rapidly and reproducibly monitor compositions of polar heteroatomic constituents, even as minor components, in a VGO, as a function of distillation temperature, with minimal sample consumption, via selective ionization without matrix effects from nonionized

(50) Yepez, O. Influence of different sulfur compounds on corrosion due to naphthenic acid. *Fuel* **2005**, *84* (1), 97−104.

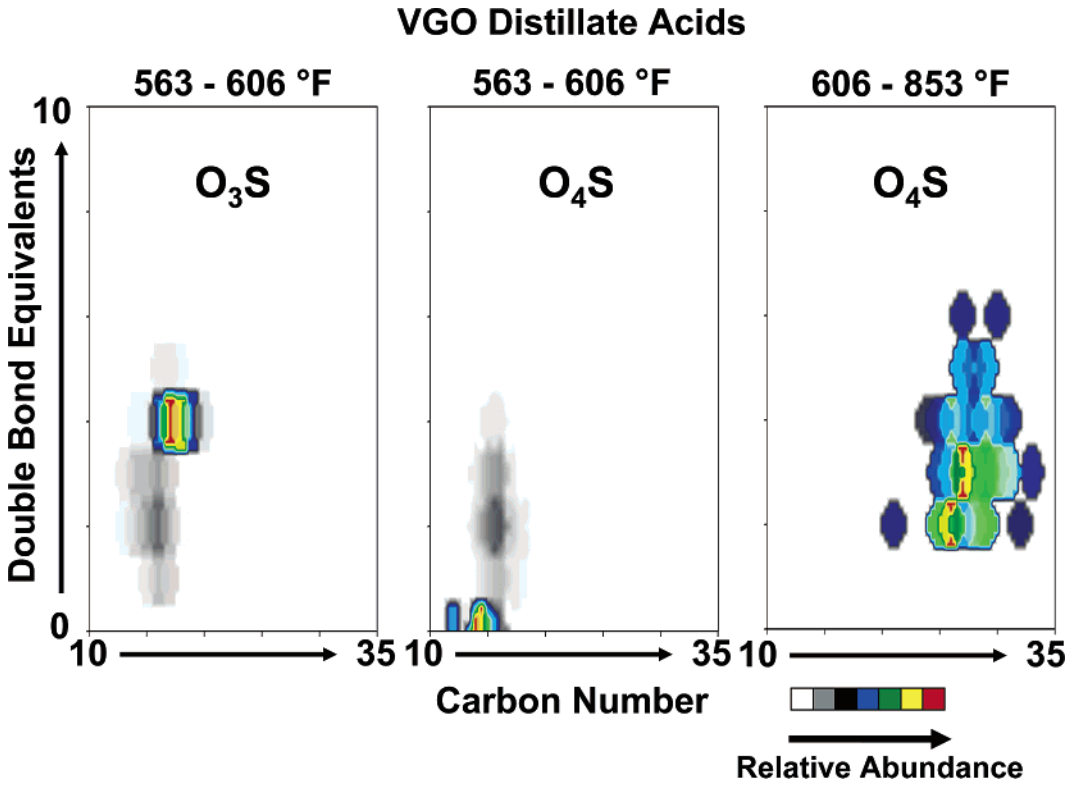

Figure 13. Three-dimensional (3D) DBE versus carbon number distribution for the negative-ion O_xS_y-class compounds for the light and middle distillates from a VGO.

species.[51] Thousands of compositions may be observed simultaneously, as well as their molecular weight, heteroatom class, aromaticity, and alkylation distributions, identified in a single positive- or negative-ion mass spectrum, without sample pretreatment.

As expected, we observed that the molecular weight, number of different elemental compositions and heteroatom classes, double-bond equivalents (DBE), and extent of alkylation increased as the distillation temperature increased. Interestingly, we observed noncovalent dimers and trimers (demonstrated by their conversion to monomers via infrared multiphoton dissociation (IRMPD)) only in the light distillate for both acidic (mostly O_2, with some O_3S and O_4S) and basic (mostly N and OS) compound classes. The presence of oxygen-containing sulfur compounds at low distillation temperature (563−606 °F) may account for the enhanced corrosivity of naphthenic acids of low total acid number (TAN). Phenolic, polyaromatic O_2, and nitrogenated species are confined to the middle and heavy distillates. Interestingly, carboxylic acids fractionate according to alkyl chain length but not by DBE value. Compound classes that distill into the middle and heavy distillate fractions exhibit class, type, and carbon number overlap with the light distillate fraction but with extended carbon number and type range for all classes. Short-chain (C_{13}−C_{26}) low-DBE (DBE < 7) O_2 species that are typically associated with corrosive behavior are not observed in the middle and heavy distillates, whereas their longer-chain, low-DBE counterparts are present in significant abundance in the middle and heavy distillates. The present compositional accounting by positive-ion and negative-ion ESI FT−ICR MS of the overlap/separation of troublesome recalcitrant or corrosive species in a VGO distilled at various temperatures should provide a rational basis for optimizing refinery processes to minimize environmental risk and refinery damage.

Acknowledgment. We thank Christopher L. Hendrickson and John P. Quinn for helpful discussions. This work was supported by the NSF National High Field Mass Spectrometry Facility (DMR 00-84173), Florida State University, and the National High Magnetic Field Laboratory in Tallahassee, FL.

EF060104G

(51) Klein, G. C.; Angström, A.; Rodgers, R. P.; Marshall, A. G. Use of Saturates/Aromatics/Resins/Asphaltenes (SARA) Fractionation To Determine Matrix Effects Crude Oil Analysis by Electrospray Ionization Fourier Transform Ion Cyclotron Resonance Mass Spectrometry. *Energy Fuels* **2006**, *20* (2), 668−672.